INTERNATIONAL JOURNAL FOR NUMERICAL METHODS IN FLUIDS
Int. J. Numer. Meth. Fluids 2009; **61**:1053–1062
Published online 5 January 2009 in Wiley InterScience (www.interscience.wiley.com). DOI: 10.1002/fld.1990

SHORT COMMUNICATION

A note on two upwind strategies for RBF-based grid-free schemes to solve steady convection–diffusion equations

Y. V. S. S. Sanyasiraju*,† and G. Chandhini

Department of Mathematics, Indian Institute of Technology Madras, Chennai 600036, India

SUMMARY

In this paper, two radial basis function (RBF)-based local grid-free upwind schemes have been discussed for convection–diffusion equations. The schemes have been validated over some convection–diffusion problems with sharp boundary layers. It is found that one of the upwind schemes realizes the boundary layers more accurately than the rest. Comparisons with the analytical solutions demonstrate that the local RBF grid-free upwind schemes based on the exact velocity direction are stable and produce accurate results on domains discretized even with scattered distribution of nodal points. Copyright © 2009 John Wiley & Sons, Ltd.

Received 15 September 2008; Revised 25 November 2008; Accepted 26 November 2008

KEY WORDS: radial basis function; multiquadric; upwind; convection–diffusion; gridfree; numerical

1. INTRODUCTION

The convection–diffusion plays a very significant role in fluid flow and heat transfer problems. This process is peculiar in the sense that it is a combination of two dissimilar phenomena, convection and diffusion. It can also be viewed as a simplified model problem to the governing equations of the fluid flow, i.e. Navier–Stokes equations. This makes numerical prediction of the solution of the convection–diffusion equation very important in computational fluid dynamics.

1.1. Convection–diffusion problems

A steady convection–diffusion equation is given by

$$\bar{a}\cdot\nabla u(\bar{x})-\mathscr{D}\nabla^2 u(\bar{x})=f(\bar{x}),\quad \bar{x}\in\Omega\subset\mathbb{R}^d \tag{1}$$

*Correspondence to: Y. V. S. S. Sanyasiraju, Department of Mathematics, Indian Institute of Technology Madras, Chennai 600036, India.

†E-mail: sryedida@iitm.ac.in

Copyright © 2009 John Wiley & Sons, Ltd.

and the general boundary conditions are

$$\alpha_1 u(\bar{x}) + \alpha_2 \nabla u(\bar{x}) = g(\bar{x}), \quad \bar{x} \in \partial\Omega \tag{2}$$

where $u(\bar{x})$ is the unknown to be computed, d is the dimension of the problem, Ω is a bounded domain in $\mathbb{R}^d$, $\partial\Omega$ is the boundary of Ω, $\mathscr{D}$ is the diffusion coefficient, $\bar{a} = (a_1, \ldots, a_d)$ is the convection coefficient, $\nabla = e_j \partial/\partial x_{e_j}$ is gradient operator, $\nabla^2 = \partial^2/\partial x_{e_j} \partial x_{e_j}$, α_1 and α_2 are known constants and $f(\bar{x})$ and $g(\bar{x})$ are some known functions.

2. RADIAL BASIS FUNCTION (RBF) APPROXIMATION OF OPERATORS

A function $\Phi : \mathbb{R}^d \to \mathbb{R}$ is called *radial* provided there exists a univariate function $\phi : [0, \infty) \to \mathbb{R}$ such that $\Phi(\bar{x}) = \phi(r)$, where $r = \|\bar{x}\|$ and $\|\cdot\|$ is some norm on $\mathbb{R}^d$. RBFs are well known for approximating multivariate functions, especially from a sparse and scattered set of data.

Kansa [1] has initiated the use of RBF interpolation in the global collocation methods for solving partial differential equations. Owing to the global nature of the method, the resultant linear system was full and highly ill-conditioned. Various approaches, namely domain decomposition, preconditioning and the use of compactly supported RBFs have been experimented to circumvent these difficulties. Recently, an RBF-based local method has been proposed by Wright and Fornberg [2]. The localization approach given in Wright and Fornberg [2] has been successfully extended by Chandhini and Sanyasiraju to steady convection–diffusion problems [3] and to unsteady incompressible Navier–Stokes equations [4]. To understand the development of the proposed upwind schemes, the local RBF scheme [3] is briefly described here.

Let $\mathscr{L}$ be the convection–diffusion operator given by $\bar{a} \cdot \nabla - \mathscr{D}\nabla^2$ and n be the total number of nodes in the discretized domain. Also assume that $\bar{x}_i$ be any point from the domain. Define $S_i = \{\bar{x}_1, \ldots, \bar{x}_{n_i}\}$ as a neighborhood of $\bar{x}_i$ consisting of $n_i (\ll n)$ nodes. To approximate $\mathscr{L}u(\bar{x}_i)$ over the nodes from S_i, let it be represented as a linear combination of u at the points of S_i, given by

$$\mathscr{L}u(\bar{x}_i) \approx \sum_{j=1}^{n_i} c_j u(\bar{x}_j) \tag{3}$$

Then, the computation of the weights c_j gives the required approximation to $\mathscr{L}u(\bar{x}_i)$. To proceed further, also consider the Lagrange representation of an interpolant $s(\bar{x})$ of $u(\bar{x})$ given by

$$s(\bar{x}) = \sum_{j=1}^{n_i} \psi_j(\bar{x}) u(\bar{x}_j) \tag{4}$$

where $\psi_j(\bar{x})$'s are the Lagrange functions that satisfy the cardinal conditions

$$\psi_j(\bar{x}_k) = \delta_{jk}, \quad j, k = 1, 2, \ldots, n_i \tag{5}$$

Applying the operator $\mathscr{L}$ to the Lagrange representation of RBF interpolant (4) gives

$$\mathscr{L}u(\bar{x}_i) \approx \mathscr{L}s(\bar{x}_i) = \sum_{j=1}^{n_i} \mathscr{L}\psi_j(\bar{x}_i) u(\bar{x}_j) \tag{6}$$

Copyright © 2009 John Wiley & Sons, Ltd.

DOI: 10.1002/fld

Comparing Equations (3) and (6), c_j's can be given as

$$c_j = \mathscr{L}\psi_j(\bar{x}_i), \quad j=1,\ldots,n_i \tag{7}$$

Therefore, to obtain each Lagrange function ψ_j in (4), an RBF based interpolation problem is developed. That is, each ψ_j is approximated as

$$\psi_j(\bar{x}) \approx \sum_{k=1}^{n_i} \lambda_{jk}\phi(\|\bar{x}-\bar{x}_k\|) + \sum_{k=1}^{l} \gamma_{jk} p_k(\bar{x}), \quad j=1,2,\ldots,n_i \tag{8}$$

where $\phi(\|\cdot\|)$ is some radial function, $\{p_j(\bar{x})\}_{j=1}^{l}$ is a basis for Π_m^d (space of all d-variate polynomials with degree $\leqslant m$) and l is the dimension of Π_m^d. The weights λ_{jk} and γ_{jk} are obtained by imposing the cardinal conditions (5) and orthogonality conditions

$$\sum_{j=1}^{n_i} \lambda_j p_k(\bar{x}_j) = 0, \quad k=1,\ldots,l \tag{9}$$

on the interpolant (8). From the interpolation problem (8)–(9), by making use of the symmetry of the interpolation matrix and some simple properties of the determinants, a general form for $\psi_j(\bar{x})$ is obtained (refer [3]) and used in Equation (7) which leads to

$$\begin{pmatrix} \mathbf{\Xi} & \mathbf{p} \\ \mathbf{p}^{\mathrm{T}} & \mathbf{0} \end{pmatrix} \begin{pmatrix} \bar{c} \\ \bar{\mu} \end{pmatrix} = (\mathscr{L}B(\bar{x}_i)) \tag{10}$$

where $\mathbf{\Xi}_{i,j} = \phi(\|\bar{x}_i - \bar{x}_j\|), i, j = 1,\ldots,n_i$, $\mathbf{p}_{i,j} = p_j(\bar{x}_i), j=1,\ldots,l$ and $i=1,\ldots,n_i$, $\bar{\mu}$, a dummy vector corresponding to the vector $\bar{\gamma}$ in (8) and $B(\bar{x})$ is given by

$$B(\bar{x}) = [\phi(\|\bar{x}-\bar{x}_1\|)\phi(\|\bar{x}-\bar{x}_2\|)\cdots\phi(\|\bar{x}-\bar{x}_{n_i}\|) \mid p_1(\bar{x})p_2(\bar{x})\cdots p_l(\bar{x})]^{\mathrm{T}} \tag{11}$$

Therefore, the weights c_j's in (3) are computed using (10) and (11). It is also clear from the development of the final linear system (10) that though it is dense, the size of (10) is only n_i, which is very much smaller than the size (n) of the global RBF collocation system. This makes the system more stable for wide range of ε. Further, only the right-hand side of (10) depends on the operator $\mathscr{L}$, for which the weights are to be computed. This optimizes the computation if weights have to be computed for many operators with the same distribution of nodes, as in the case of non-linear equations.

Franke [5] has made a comprehensive comparison of about seven groups consisting of about 30 interpolation methods on six different test functions and found that performance of multiquadric (MQ) is the most impressive and consistently performed better in terms of accuracy. Therefore, the MQ function developed by Hardy [6] and defined as

$$\Phi(\bar{x}) = \sqrt{1+\varepsilon^2\|\bar{x}\|^2} \tag{12}$$

where $\varepsilon > 0$ has been used in all the computations presented in the subsequent sections.

The numerical computation of the solution of the convection–diffusion problem, described in (1)–(2) using the above described RBF method, becomes very challenging, like any other conventional methods, when the convective process is dominant over diffusion. That is, the dimensionless parameter that measures the relative strength of the diffusion ($\mathscr{D}$) over convection is very small.

Copyright © 2009 John Wiley & Sons, Ltd.

In such situations, numerical approximations get contaminated due to the spurious oscillations and numerical diffusion. Upwind approximation is one of the important concepts, which has been used in the conventional schemes such as finite difference, finite element and finite volume methods to suppress the ‘wiggles’ when convection is dominant. All upwind techniques take into account the direction of the velocity. It is known that in a strong convective problem, the center node receives more influence from the upstream side than from the downstream. Therefore, in one-dimensional problems, optimal upwinding is straightforward to implement as the velocity, either positive or negative, is always in the coordinate direction. However, the implementation is very complex in multi-dimensional problems. Conventionally, the upwind concept in multi-dimensional problems is implemented independently for each coordinate direction. That is, the partial derivatives are approximated in each coordinate direction independently over a set of nodes chosen based on the sign of the velocity component of that particular direction. However, such upwind techniques are prone to crosswind diffusion.

3. UPWIND SCHEMES BASED ON THE EXACT VELOCITY DIRECTION

It is evident that, in higher-dimensional problems, the sense of the vector $\bar{a}$ in (1) need not coincide with any particular coordinate direction. This suggests that the computational molecule over which the upwind has to be applied should be chosen based on the exact velocity direction and not by separately looking at the velocity components. Therefore, designing upwind schemes for multi-dimensional problems is not straightforward for the classical grid-based schemes such as finite difference, finite element or finite volume. Owing to the grid-free nature of the RBF local scheme [3], it is possible to incorporate the upwind strategy effectively in the actual velocity direction. In the sections to follow, two upwind techniques based on the exact velocity direction have been presented and their validation over some convection-dominated convection–diffusion problems is also demonstrated.

3.1. Upwind scheme-I (U-I)

In this scheme, only the upwind nodes from the local support domain, S_i for each nodal point $\bar{x}_i$, are used to approximate the derivatives. The upwind nodes are the upstream nodes from the support domain selected by taking a line passing through the point $\bar{x}_i$ and normal to the velocity vector. That is, as given in Figure 1(a), nodes denoted by ‘$\circ$’ in the support domain of $\bar{x}_i$ are chosen to approximate the derivatives.

3.2. Upwind scheme-II (*U-II*)

For moderate values of the diffusion coefficient $\mathscr{D}$ as given in (1), the central support (points are chosen from all directions) gives good results, but deviates substantially from the exact solution for small values of $\mathscr{D}$. By taking this into account an adaptive upwind scheme has been used, in which the local support for the node $\bar{x}_i$ is shifted in the opposite direction of the flow as shown in Figure 1(b). This local shift has been implemented adaptively based on the value of the local Peclet number $\bar{P}e = \bar{a}dc/\mathscr{D}$, where $\bar{a}$ is the velocity vector and dc the average nodal spacing. Depending on the magnitude of the local Peclet number at the node $\bar{x}_i$, the corresponding support domain will be shifted toward the upwind direction. Since the upstream direction, $\bar{\gamma}_i$, is the opposite direction of $\bar{a}$, it can be computed by taking $\bar{\gamma} = -\bar{a}/\|a\|$. Then the local support domain is shifted to a distance

Copyright © 2009 John Wiley & Sons, Ltd.

DOI: 10.1002/fld

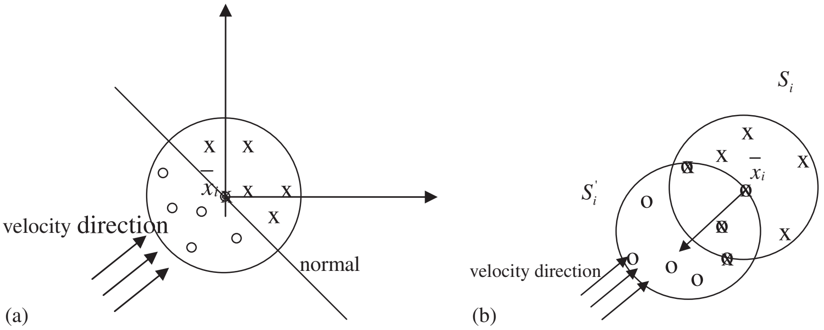

Figure 1. Local support for: (a) upwind scheme-I and (b) upwind scheme-II.

ds in the direction $\bar{\gamma}$. The distance ds is computed using $\mathrm{ds}=\beta\cdot r$, where $\beta=\coth\|\bar{Pe}\|-1/\|\bar{Pe}\|$ and r is the radius of the support domain. It can be seen from the definition of β that

$$\begin{aligned}\beta &\to 0 \quad \text{as } |\bar{Pe}|\to 0\\ \beta &\to 1 \quad \text{as } |\bar{Pe}|\to\infty\end{aligned} \tag{13}$$

Therefore, for large values of Peclet numbers, the proposed upwind scheme chooses a full upwind support domain (the magnitude of the shift ds is equal to the radius of the central support domain). On the other hand for small and moderate values of the local Peclet number, the magnitude of the shift ds will be between zero and r (radius of the central support domain). This makes the support domain, for each node $\bar{x}_i$, adaptive. A similar upwind scheme was used by [7]; however, the interest there was to apply the same in polynomial point collocated method and concluded that the scheme works well when large number of grid points were used. The purpose of the present scheme is to make it local by minimizing the number of nodes in the local support domain S_i.

3.3. Numerical implementation

To discretize the convection–diffusion equation (1) at each node $\bar{x}_i, i=1,\dots,n$

1. Start with a central support S_i where the nodes are chosen from all directions with equal weightage.
2. Find the upwind support domain S_i' from the central support domain S_i using the procedure U-I or U-II.

Procedure U-I

- Find the normal to the vector $\bar{a}$ which passes through $\bar{x}_i$.
- Select the nodes on the upstream side to the normal from S_i and store them in S_i'.
- Discretize the convection part $\bar{a}\cdot\nabla$ over the support S_i' and compute the weights c_j' by solving the linear system in (10).
- Discretize the diffusion part ∇^2 over the support S_i and again compute the weights c_j'' by solving the linear system in (10).
- The weights for the full convection–diffusion operator c_j are then obtained by $c_j=c_j'+c_j''$ if $\bar{x}_{i_j}\in S_i$ or $c_j=c_j''$ if $\bar{x}_{i_j}\in S_i'$.

Copyright © 2009 John Wiley & Sons, Ltd.

DOI: 10.1002/fld

Procedure U-II

- Compute
  - The local Peclet number, $\bar{Pe} = \bar{a}dc/\mathscr{D}$
  - Upstream direction $\bar{\gamma} = -\bar{a}/\|a\|$
  - The distance $\mathrm{ds} = \beta \cdot r$, where $\beta = \coth\|\bar{Pe}\| - 1/\|\bar{Pe}\|$
- Select the upwind support domain S_i' with a center node $\bar{x}_i'$, where $\bar{x}_i'$ is at a distance ds in the direction $\bar{\gamma}$ from the node $\bar{x}_i$.
- Compute the weights c_j for the full convection–diffusion operator using the support S_i'.

After computing the weights using the above-mentioned procedure, the resultant algebraic system is solved using any direct or iterative method.

4. RESULTS AND DISCUSSION

In this section, numerical results obtained using the RBF local scheme with the proposed upwind techniques U-I and U-II for linear convection–diffusion problems have been analyzed. To demonstrate the implementation of the grid-free upwind schemes in multi-dimensional problems, two dimensional equivalents of (1) have been chosen. MQ RBF has been used in all the simulations and the shape parameter ε has been varied to observe its effect on the accuracy of the solutions. The example problems have been defined over a unit square and both uniform and scattered nodal distributions, as shown in Figure 2, are used to obtain the solutions. The number of supporting nodes in S_i has been fixed as $n_i = 5$ for both the distributions. A standard 5-point stencil has been considered for the uniform case, whereas in the case of scattered distribution, nodes are chosen by fixing the radius of the support. The radius has been fixed such that a minimum of five nodes survive in the neighborhood of every centre node, $\bar{x}_i$. The results obtained have been compared with the results of the conventional upwind method, hereafter denoted as U-0, wherein the upwind is based on the sign of the velocity component for each coordinate direction independently. For

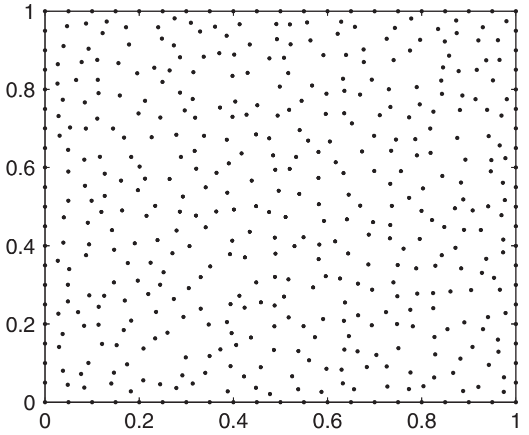

Figure 2. Scattered distribution of 480 nodes.

example, when kth component of $\bar{a}$ (at $\bar{x}_i$) >0, i.e. $a_k>0, k=1,\dots,d$, $\bar{x}_j\in S_i$ is chosen to be in the upwind support, if $x_{jk}<x_{ik}, k=1,\dots,d$ (vice versa for $a_k<0$). The error in the approximate solution with respect to analytical solution has been computed using ∞-norm (err_∞) which is given by

$$\mathrm{err}_\infty=\max(|u_i^{\mathrm{approx}}-u_i^{\mathrm{anal}}|, i=1,\dots,n) \tag{14}$$

Three model problems, two with constant and another with variable velocity components, have been chosen for the purpose of validation. For all the problems, the boundary conditions and the source terms f are taken from the corresponding analytical solutions.

4.1. Example

Consider the problem (1)–(2) with $\bar{a}=(1,0)$ and analytical solution

$$u(x,y)=\mathrm{e}^{x/2\mathscr{D}}\sin\pi y[2\mathrm{e}^{-1/2\mathscr{D}}\sinh\sigma x+\sinh\sigma(1-x)]/\sinh\sigma \tag{15}$$

where $\sigma^2=\pi^2+0.25/\mathscr{D}^2$.

In Example 4.1, the y-component of the velocity vector $\bar{a}$ is zero and hence the direction of the velocity field is parallel to the x-axis. Therefore, the upwind schemes U-0 and U-1 coincide with each other and produce identical results.

The solutions are obtained by varying global Peclet numbers (Pe_g) defined by $Pe_\mathrm{g}=Ul/\mathscr{D}$, where U is the characteristic velocity and l is the characteristic length (h for uniform and dc for scattered nodal distributions). Figure 3 compares the errors with respect to the global Peclet numbers for the three upwind techniques U-0, U-I and U-II. The error plots with uniform and scattered nodal distributions are included in this figure as (a) and (b), respectively. As expected the error plots for U-0 and U-1 coincide with both uniform and scattered nodal distributions. However, the corresponding plot with U-II has some very interesting features. It is clear from Figure 3(a), that for the computations over uniform nodal distribution, the scheme U-II gave more accurate solutions over the other two until Pe_g is about 50. But, for large Pe_g the upwind schemes U-0 and U-I seem to be more accurate. However, the accuracy improved substantially with the scheme U-II for small Peclet numbers Pe_g, which can be achieved by reducing the step length. One of the main reasons for this improvement in the accuracy of the solution is due to the adaptive nature of U-II.

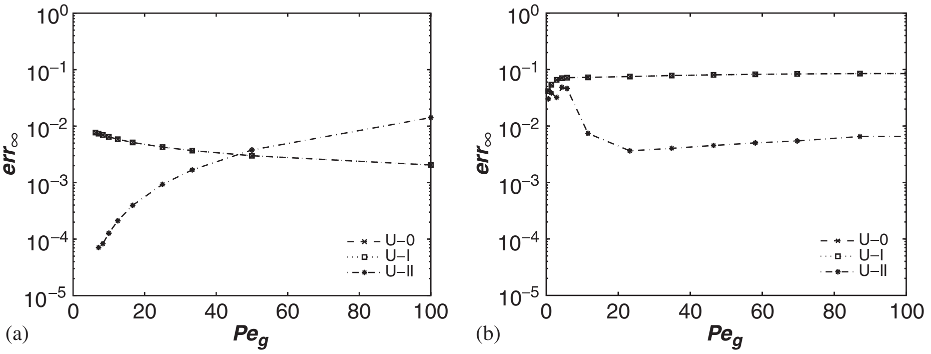

Figure 3. Comparison of error plots for Example 4.1: (a) Uniform and (b) Scattered nodal distributions.

Copyright © 2009 John Wiley & Sons, Ltd.

DOI: 10.1002/fld

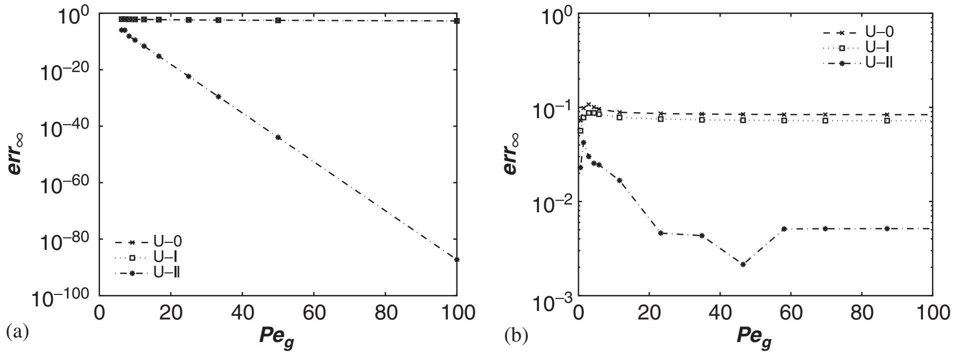

Figure 4. Comparison of error plots for Example 4.2: (a) Uniform and (b) Scattered nodal distributions.

In Figure 3(b) error plots with respect to Pe_{g} are presented. In these computations, the scattered nodal distribution shown in Figure 2 has been used. For the scattered case, clearly, U-II dominates over the other two upwind techniques by showing a substantial improvement in the solution as Pe_{g} increases. In this case, near optimal shape parameter ($\varepsilon_{\mathrm{opt}}$) has been used for all values of Pe_{g}. For example, $\varepsilon = 10$, 50 and 5.5 are found to be optimal for $Pe_{\mathrm{g}} = 0.58$, 5.8 and 58, respectively.

4.2. *Example*

In this example, parameter $\bar{a}$ has been chosen as $(-2, 2)$ with analytical solution

$$u(x, y) = [\mathrm{e}^{2(1-x)/\mathscr{D}} + \mathrm{e}^{2y/\mathscr{D}} - 2]/(\mathrm{e}^{1/\mathscr{D}} - 1) \tag{16}$$

The error plots by varying Pe_{g} are presented in Figure 4 for both uniform and scattered nodal distributions. In this case, the results obtained using U-II are highly superior to the other two upwind schemes U-0 and U-I when uniform nodes have been used. For example, with $n = 11 \times 11$, err_∞ with U-II is about 10(−86) (read as 10^{-86}), whereas the corresponding errors using U-0 and U-I are in the order of 10(−05). In this example also, both U-0 and U-I solutions are almost same for the uniform case, though the support domains need not be the same. This coincidence in the solution may be due to the use of uniform distribution of the nodes. For scattered node distribution, Example 4.2 also shows a similar trend in the accuracy of the solution, as that of Example 4.1 for U-0 and U-II. However, the solution obtained using U-I is slightly better than U-0 and the accuracy of U-I is between U-0 and U-II. These two examples demonstrate that the scheme U-II (adaptive local support domain) is an effective method compared with U-0 and U-I to solve the convection-dominated problems.

To analyze the upwind schemes further, a third example has been chosen with a variable velocity field unlike the other two problems.

4.3. *Example*

Consider the problem with variable coefficient $\bar{a} = (\sin x, \cos x)$ with analytical solution

$$u(x, y) = \mathrm{e}^{-1/\mathscr{D}} \left[\sinh \frac{1-x}{\mathscr{D}} \sin y + \sinh \frac{1-y}{\mathscr{D}} \sin x \right] \tag{17}$$

Copyright © 2009 John Wiley & Sons, Ltd.

DOI: 10.1002/fld

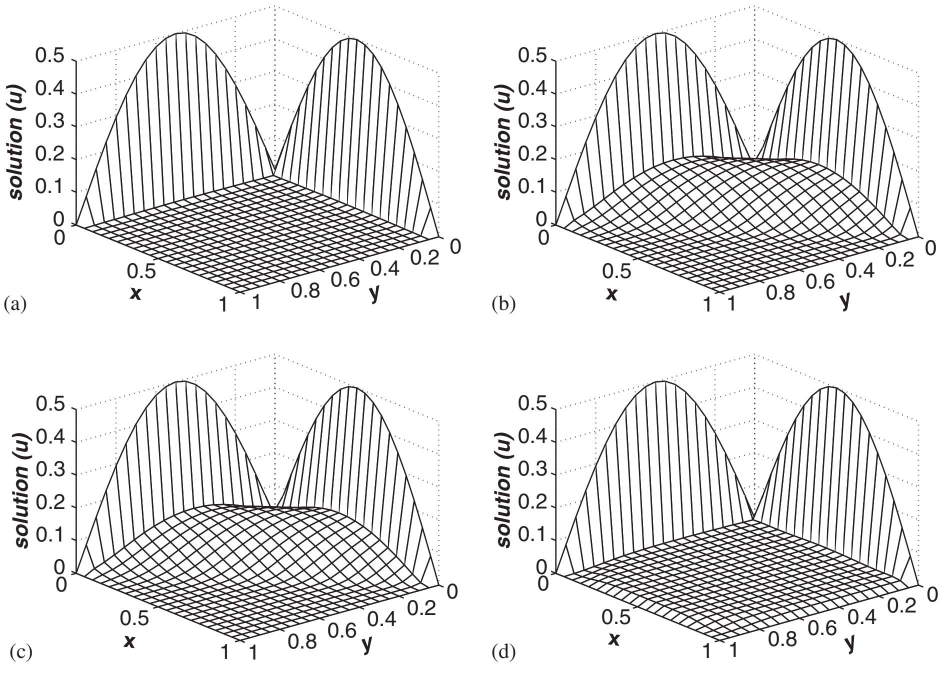

Figure 5. Surface plots of the solutions for Example 4.3: (a) exact solution; (b) U-0; (c) U-I; and (d) U-II.

Boundary conditions and the source term f have been taken from the analytical solution (17). In Example 4.3, the solutions, using all three techniques U-0, U-I and U-II, have been obtained for $\mathscr{D}=0.001$ and the corresponding solutions are presented in the Figure 5. It is very interesting to note that the upwind scheme U-II is able to resolve the boundary layer very accurately when compared with the other two. Figure 6 compares the err$_\infty$ obtained with U-0, U-I and U-II. The better accuracy with U-II, particulary when the nodal distribution is finer, is again reflected in these error plots.

5. CONCLUSIONS

To deal with the convection-dominated problems, two upwind schemes based on the exact velocity field have been compared and validated over various two-dimensional examples problems. Advantage of the RBF scheme as a pure grid-free local scheme has been exploited to incorporate the different upwind strategies effectively. The results obtained using these techniques show that the adaptive upwind technique U-II gives better accuracy and is able to resolve the boundary layers more accurately than the other two. The improvement in the accuracy of the solutions using U-I over U-0 is marginal. The concept used in the scheme U-II to make it adaptive is simple and straightforward to adopt for multi-dimensional problems. Further, it has been observed that the

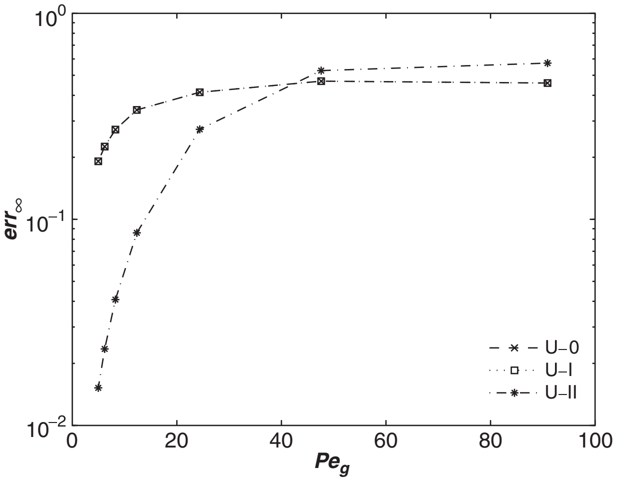

Figure 6. Comparison of error plots for Example 4.3.

accuracy also depends on RBF shape parameter ε. However, a systematic approach for the optimal choice of ε is still an open problem, though some heuristic approaches exist to date.

REFERENCES

1. Kansa EJ. Multiquadrics—a scattered data approximation scheme with applications to computational fluid dynamics. II. Solutions to parabolic, hyperbolic and elliptic partial differential equations. *Computers and Mathematics with Applications* 1990; **19**(8–9):147–161.
2. Wright GB, Fornberg B. Scattered node compact finite difference-type formulas generated from radial basis functions. *Journal of Computational Physics* 2006; **212**(1):99–123.
3. Chandhini G, Sanyasiraju YVSS. Local RBF–FD solutions for steady convection–diffusion problems. *International Journal for Numerical Methods in Engineering* 2007; **72**(3):352–378.
4. Sanyasiraju YVSS, Chandhini G. Local radial basis function based gridfree scheme for unsteady incompressible viscous flows. *Journal of Computational Physics* 2008; **227**:8922–8948.
5. Franke R. Scattered data interpolation: test of some methods. *Mathematics of Computation* 1982; **48**:181–200.
6. Hardy RL. Multiquadric equations of topography and other irregular surfaces. *Journal of Geophysical Research* 1971; **76**:1905–1915.
7. Gu YT, Liu GR. Meshless techniques for convection dominated problems. *Computational Mechanics* 2006; **38**:171–182.

Copyright © 2009 John Wiley & Sons, Ltd.

DOI: 10.1002/fld